3-77

Dr 667
UCRL-52172

TIME-DOMAIN MODELING OF NONLINEAR LOADS

J. A. Landt, E. K. Miller, and F. J. Deadrick

September 29, 1976

Prepared for U.S. Energy Research & Development Administration under contract No. W-7405-Eng-48

MASTER

NOTICE

This report was prepared as an account of work sponsored by the United States Government. Neither the United States nor the United States Energy Research & Development Administration, nor any of their employees, nor any of their contractors, subcontractors, or their employees, makes any warranty, express or implied, or assumes any legal liability or responsibility for the accuracy, completeness or usefulness of any information, apparatus, product or process disclosed, or represents that its use would not infringe privately-owned rights.

NOTICE

Reference to a company or product name does not imply approval or recommendation of the product by the University of California or the U.S. Energy Research & Development Administration to the exclusion of others that may be suitable.

Printed in the United States of America
Available from
National Technical Information Service
U.S. Department of Commerce
5285 Port Royal Road
Springfield, VA 22161
Price: Printed Copy $: Microfiche $3.00

Page Range	Domestic Price	Page Range	Domestic Price
001–025	$ 3.50	326–350	10.00
026–050	4.00	351–375	10.50
051–075	4.50	376–400	10.75
076–100	5.00	401–425	11.00
101–125	5.50	426–450	11.75
126–150	6.00	451–475	12.00
151–175	6.75	476–500	12.50
176–200	7.50	501–525	12.75
201–225	7.75	526–550	13.00
226–250	8.00	551–575	13.50
251–275	9.00	576–600	13.75
276–300	9.25	601–up	*
301–325	9.75		

*Add $2.50 for each additional 100 page increment from 601 to 1,000 pages; add $4.50 for each additional 100 page increment over 1,000 pages.

Distribution Category
UC-34

LAWRENCE LIVERMORE LABORATORY
University of California Livermore, California 94550

UCRL-52172

TIME-DOMAIN MODELING OF NONLINEAR LOADS

L. A. Landt*, E. K. Miller,
and F. J. Deadrick

MS. Date: September 29, 1976

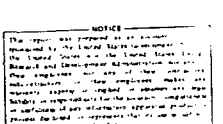

*Los Alamos Scientific Laboratory.

TIME-DOMAIN MODELING OF NONLINEAR LOADS

Abstract

The behavior of an antenna or scatterer when loaded with a nonlinear impedance can be changed greatly from that observed under linear conditions. In some cases, the nonlinearity causes detrimental effects such as the intermodulation products arising from the nonlinear mixing of two frequencies. In other cases, the nonlinearity may be exploited profitably, e.g., to reduce late-time ringing on a pulse-excited antenna.

In this report, we describe and illustrate a procedure for treating general nonlinear loads. We also apply this procedure through a computer program, to several specific types of nonlinearities. We develop the treatment within the framework of the thin-wire approximation to the electric-field integral equation. As such, the treatment can be applied to the large class of objects modeled by wires.

The nonlinear load types that we consider include those with piecewise-linear voltage-current curves (e.g., one or more diodes), a load with a time-varying impedance (which permits modulating the fields scattered from it), and a general nonlinear load represented by specified voltage-current functions.

Introduction

Recent developments in direct procedures for solving time-domain problems now make it possible to treat some nonlinear problems of interest in electromagnetics. An example is the work of Merewether.[1,2] He uses the differential form of Maxwell's equations and a finite-difference numerical treatment to examine the transient currents on a conducting body located in a nonlinear plasma medium.

An alternate, integral-equation treatment has been developed by Schuman,[3] Liu and Tesche,[4] and Sarker and Wetner[5] to study the influence of a nonlinear load on the behavior of a linear wire antenna. The integral-equation approach is the one we follow here. However, it differs in type from that used in Ref. 4, and it differs in numerical treatment from that utilized in Ref. 3. Also, it offers a more general method for analyzing nonlinearly loaded wire objects.

Formulation and Numerical Treatment

The integral equation of interest[6] can be written as

$$\hat{s} \cdot \bar{E}^{INC}(\bar{r},t) = \frac{\mu_0}{4\pi} \int_{C(\bar{r})} \left[\frac{\hat{s} \cdot \hat{s}'}{R} \frac{\partial}{\partial t'} I(s',t') + c \frac{\hat{s} \cdot \bar{R}}{R^2} \frac{\partial}{\partial s'} I(s',t') - c^2 \frac{\hat{s} \cdot \bar{R}}{R^3} q(s',t') \right] ds', \qquad (1)$$

where

$\bar{E}^{INC}(\bar{r},t)$ = incident electric field at observation point $\bar{r}$ at time t

$\hat{s}$ and $\hat{s}'$ = unit vectors parallel to $C(\bar{r})$ at $\bar{r}$ and $\bar{r}'$

c = velocity of light

μ_0 = permeability of free space

$I(s',t')$ and $q(s',t')$ = current and charge, respectively, at point s' and retarded time $t' = (t - \frac{R}{c})$, where $R = |\bar{r} - \bar{r}'|$

$C(\bar{r})$ = structure contour, assumed for now to be perfectly conducting.

Solving (1) numerically by the method of moments (using in this case point matching and a 9-point Lagrangian interpolation scheme for the currents at space point $\bar{r}_i$, $i = 1,\ldots,N$ and time step t_j, $j = 1,\ldots,M$) reduces to the linear form:*

$$E^{SCA}_{ij} + E^{INC}_{ij} = Z_{ii'} I_{i'j}; \quad i,i' = 1,\ldots,N, \quad j = 1,\ldots,M,$$

where

$E^{SCA}_{ij} = E^{SCA}(\bar{r}_i,t_j)$, the tangential scattered field at observation point $\bar{r}_i$ and time step t_j due to currents at earlier time $t_{j'}$, $j' < j$

$E^{INC}_{ij} = \hat{s}_i \cdot \bar{E}^{INC}(\bar{r}_i,t_j)$

$I_{i'j} = I(\bar{r}_{i'},t_j)$

---

*Indices for a space-sampled quantity are i and k, while j is used for a time-sampled index.

and summation over repeated indices is assumed. Quantity $Z_{ii'}$ is a time-independent interaction matrix that relates the current sample value $I_{i'j}$ at the present time step to the sum of the exciting field and the field scattered from other parts of $C(\bar{r})$. Because interaction between current values at different space points is permitted in the treatment by the interpolation scheme we used, $Z_{ii'}$ is not diagonal although, in general, it will be sparse and diagonally dominant.

Note that E^{SCA}_{ij} can also be expressed in terms of an impedance matrix $Z_{ii'}$ as

$$E^{SCA}_{ij} = Z_{ii'} I_{i'j'} ,$$

where

$$j' = j - R_{ii'}/c\delta$$

with $R_{ii'} = |r_i - r_{i'}|$, δ is the solution time-step size, and j' is rounded off to integer value.

Thus, we are able to obtain

$$I_{ij} = Y_{ii'} \left[E^{SCA}_{i'j} + E^{INC}_{i'j} \right] , \tag{2}$$

where

$$\bar{\bar{Y}} = \bar{\bar{Z}}^{-1}$$

Using (2) we can then develop a solution for the induced current, from the specified $E^{INC}_{i'j}$, as a time-stepping procedure from an initial value problem.

When the structure is loaded with a linear impedance, (2) can be expressed as

$$I_{ij} = Y_{ii'} \left[E^{SCA}_{i'j} + E^{INC}_{i'j} + Z^{L}_{i'k} I_{kj'} \right] \tag{3}$$

with $Z^L_{i'k}$, the load impedance matrix, which could in general contain both self-terms and mutual terms. For the special case of a single, self-impedance lumped load at i = L, we obtain from (3):

$$I_{Lj} = Y_{Li'} \left[E^{SCA}_{i'j} + E^{INC}_{i'j} \right] - Y_{LL} Z^L_{LL} I_{Lj} \quad , \tag{4a}$$

$$I_{ij} = Y_{ii'} \left[E^{SCA}_{i'j} + E^{INC}_{i'j} \right] - Y_{iL} Z^L_{LL} I_{Lj'}$$

$$= Y_{ii'} \left[\tilde{E}^{SCA}_{i'j} + E^{INC}_{i'j} \right] \; ; \quad i \neq L \tag{4b}$$

where

$$\tilde{E}^{SCA}_{i'j} = E^{SCA}_{i'j} - \delta_{iL} Z^L_{LL} I_{Lj'} \quad ,$$

with δ_{iL} the Kronecker delta function.

The j' subscript appears in the $I_{Lj'}$ term because the spatial separation between the load point and the other current sample points delays the term's effect by the time R_{iL}/c.

We observe that: the only explicit effect of the load is its appearance in the equation that specifies the current through the load; the other current values are implicitly affected through $\tilde{E}^{SCA}_{i'j}$ as the fields resulting from I_{Lj} propagate outward; and

$$I_{Lj} = \frac{Y_{Li'} \left[E^{SCA}_{i'j} + E^{INC}_{i'j} \right]}{1 + Y_{LL} Z^L_{LL}} \quad , \tag{5}$$

which is analogous to the corresponding result for frequency domain.

Note that if the self-impedance loading is linear but distributed, the result is not much more involved than (5) and it leads to

$$I_{ij} = Y^L_{ii'} \left[E^{SCA}_{i'j} + E^{INC}_{i'j} \right] \quad , \tag{6}$$

where

$$Y^L_{ii'} = \left(Z_{ii'} + \delta_{ii'} Z^L_{ii} \right)^{-1} \quad .$$

For the case of a single nonlinear load, (4) is formally the same. But we now identify a time-dependent load Z^L_{LLj}, given by

$$Z^L_{LLj} = Z^L_{LL}(I_{Lj}) \text{ or } Z^L_{LLj} = Z^L_{LL}(t_j) \tag{7}$$

whose functional form is yet to be given. Equation (5) still applies, but the formal dependence of Z^L_{LLj} upon the current, or time, leads to

$$I_{Lj} = \frac{Y_{Ll'}\left[E^{SCA}_{l'j} + E^{INC}_{l'j}\right]}{1 + Y_{LL}Z^L_{LLj}} \tag{8}$$

so that the numerical solution for I_{Lj} requires that (7) and (8) be simultaneously satisfied.

Observe that in writing Z^L_{LLj} in the forms given by (7), we have allowed for two distinct types of load variations: a nonlinear dependency of Z^L_{LLj} upon I_L, and a time-varying Z^L_{LLj} that is independent of I_L. Examples of the former are a diode rectifier and square-law detector. An example of the latter could result from applying a separate modulation voltage to a diode. (Some results for these two load types are included in the next section.)

It is worthwhile mentioning that the current through a single load, linear or nonlinear, can also be written in terms of its no-load or short-circuit value as[4]:

$$I_{Lj} = I^{SC}_{Ll} - \tilde{Y}_{LL,j-j'} Z^L_{LL} I_{Lj'} \; ; \quad j' = 1,\ldots,j$$

where $\tilde{Y}_{LL,j-j'}$ is the inverse Laplace transform of the short-circuit input admittance of the antenna at the position of the load.

Numerical Results

Our purpose here is to demonstrate the nonlinear analysis capability, described above, for various possible applications. We present sample results for problems in both radiation and scattering. The load types we consider are those that exhibit nonlinear, voltage-current (V-I) behavior and a time-dependent impedance. Where convenient, we have chosen examples that seem relevant to practical problems of current concern, e.g., EMP (electromagnetic pulse) protection devices.

The current and charge distributions on a 1-m dipole antenna for several time periods are shown in Fig. 1. The antenna, which had an ideal diode (0 Ω forward resistance, 100 kΩ reverse) at its center, was excited by a Gaussian voltage pulse. Also, Fig. 1 shows the source-segment current and the broadside radiated field as a function of time. The induced current may be of interest in applications where the radiated field is used in pulse shaping, radar cross-section (RCS) modification, etc. [e.g., EMP and EMC (electromagnetic compatibility)].

Initially, the current is identical to that for the no-load case, because the flow is in the forward direction through the diode. However, beyond the point where the current would change sign, a distinct departure from the no-load case occurs. Of particular interest is the static charge distribution, which eventually results from the large value of reverse resistance across the diode.

Another example that involves ideal diodes is illustrated in Fig. 2. Here, a 1-m dipole is again excited by a Gaussian pulse, but it is now loaded with 60 ideal diodes, one for each segment of the numerical model. The current through the source segment is again Gaussian as in Fig. 1. But the radiated far field approximates a Gaussian derivative, in contrast to the situation depicted in Fig. 1 where the late-time field had a ringdown frequency of about twice the fundamental frequency of c/2L. The changed far field is caused by the charge being trapped by the diode loads, resulting in a radiation pulse that occurs when the charge initially accelerates and when it decelerates (due to reflection) at the end. This example illustrates the potential of employing nonlinear diode loads for pulse shaping.

Results of the broadside incidence of a Gaussian pulse are shown in Fig. 3. The pulse was scattered from a 21-m dipole antenna, which had diode-type loads at its center with forward/reverse resistance values of $10/10^5$, $10/10^3$, and $10/10$ Ω. The backscattered field is shown as a function of time together with the corresponding frequency spectrum. Note the upward shift in frequency of the first backscatter resonance as the load's backward resistance is increased.

Figure 4 exemplifies the results of loading a 9-m dipole at its center with a nonlinear resistor ($R \propto 1/|V|$) and exciting it as an antenna. In (a) through (c), we observe the generation of a third harmonic of the 16-MHz

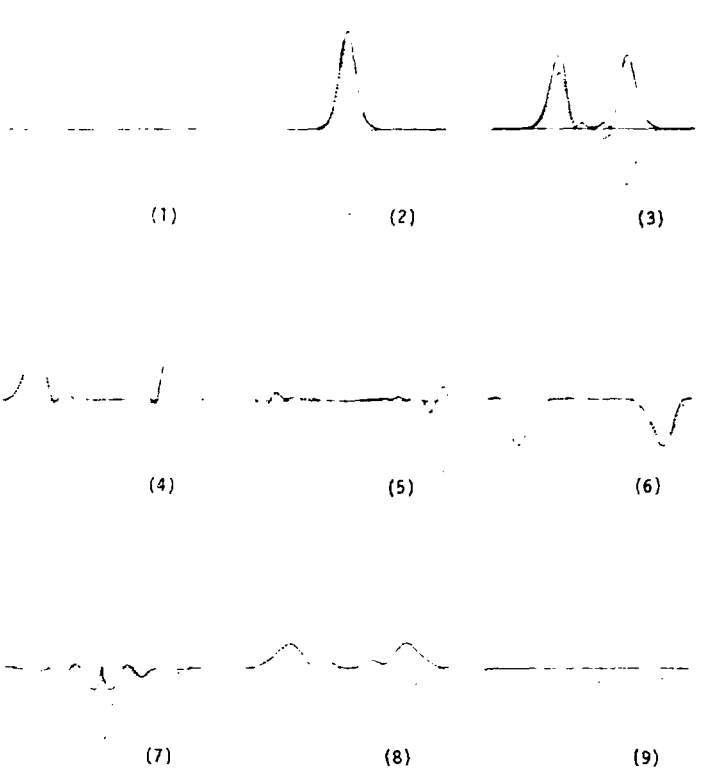

Fig. 1. Nonlinear loads in the time domain. (a) Current (——) and charge (·····) distributions on a 1-m centerfed dipole having a diode load in series with the generator. The diode presents zero impedance only to the current flowing in the initial direction, and it effectively acts as an open circuit in the opposite direction (impedance 100 kΩ). Thus, the two halves of the dipole retain a static charge distribution at late times. (b) Comparison of the transient feedpoint current for the diode load and no load. (c) Comparison of radiated field showing a fundamental frequency twice that of an unloaded dipole.

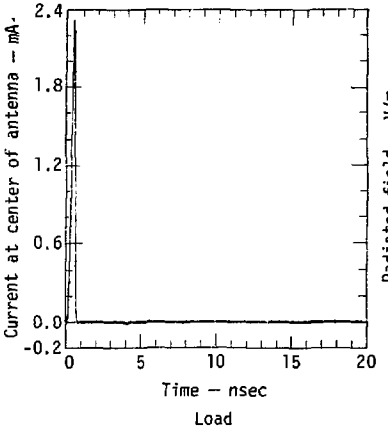
Current at center of antenna – mA
2.4
1.8
1.2
0.6
0.0
-0.2
0
5
10
15
20
Time – nsec
Load

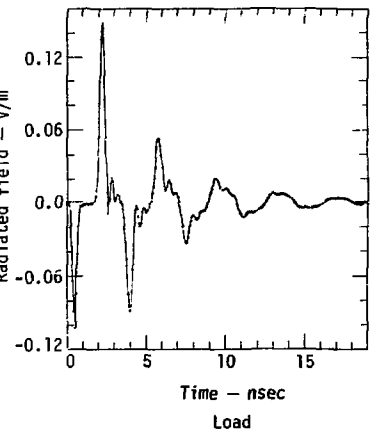
Radiated field – V/m
0.12
0.06
0.0
-0.06
-0.12
0
5
10
15
Time – nsec
Load

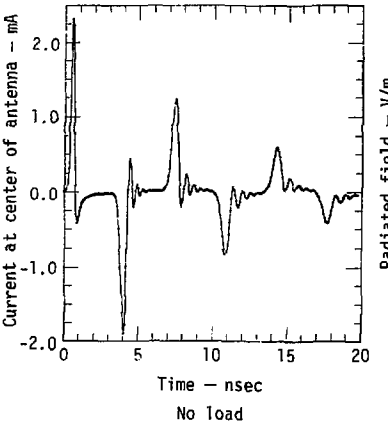
Current at center of antenna – mA
2.0
1.0
0.0
-1.0
-2.0
0
5
10
15
20
Time – nsec
No load

(b)

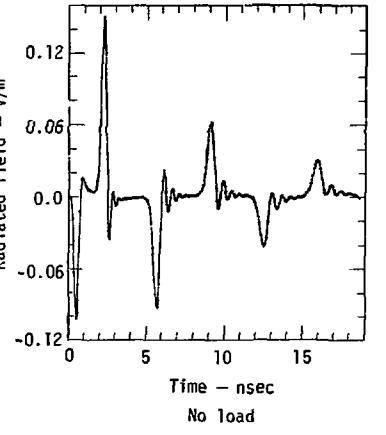
Radiated field – V/m
0.12
0.06
0.0
-0.06
-0.12
0
5
10
15
Time – nsec
No load

(c)

Fig. 1 (cont.)

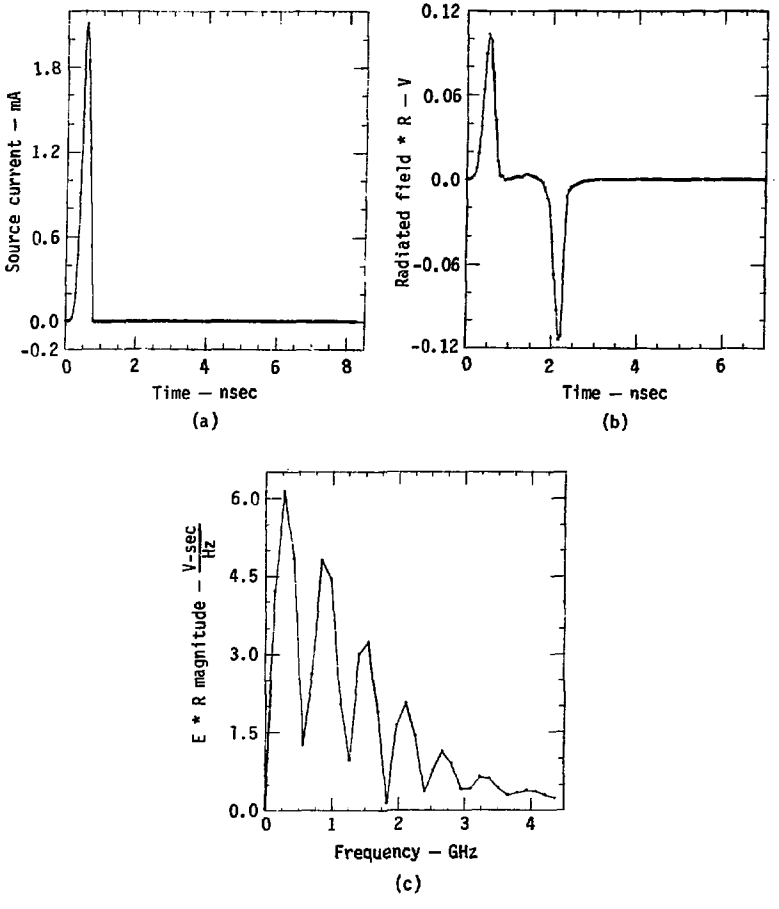

Fig. 2. Potential for pulse shaping, using nonlinear distributed loading. A 1-m dipole, modeled numerically by 60 segments, is loaded with a series of ideal diodes, one per segment. (a) Application of a Gaussian voltage pulse across the center segment produces this feedpoint current. (b) Broadside radiated field. (c) Frequency spectrum. Note the sharply curtailed time response of the field caused by the diodes and the absence of late-time ringing.

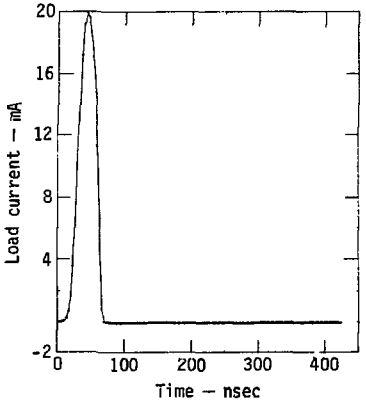

(a) Load current vs time ($10/10^5\Omega$ forward/reverse resistance)

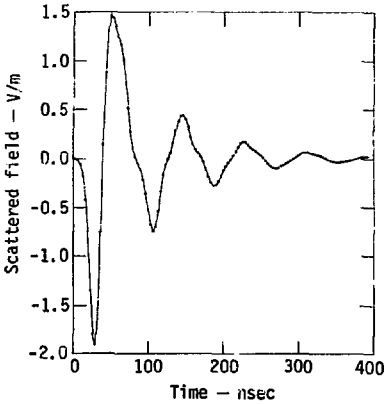

(b) Radiated field vs time ($10/10^5\Omega$ forward/reverse resistance)

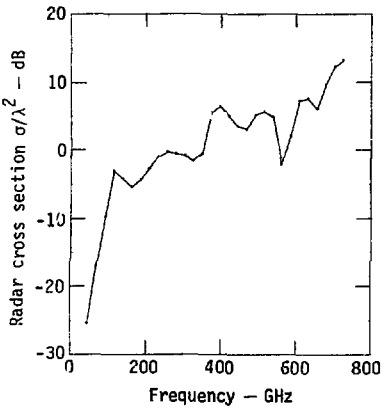

(c) σ/λ^2 vs frequency ($10/10^5\Omega$ forward/reverse resistance)

Fig. 3. Effect of the ratio of a variable forward-to-reverse diode resistance on fields scattered from a center-loaded 21-m dipole for broadside incidence of a Gaussian pulse. Note a smoothing of the frequency spectrum of the scattered field and an increase in frequency of the lowest order resonance, as the reverse resistance increases. At the largest resistance value, the wire is behaving essentially as two dipoles of half the le gth of the wire.

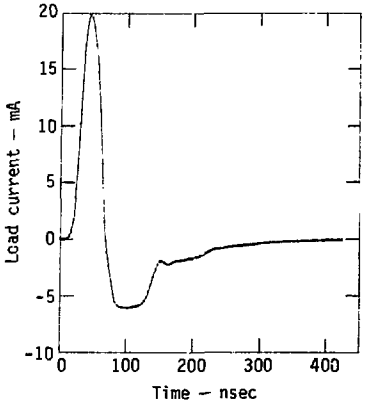

(d) Load current vs time ($10/10^3\Omega$ forward/reverse resistance)

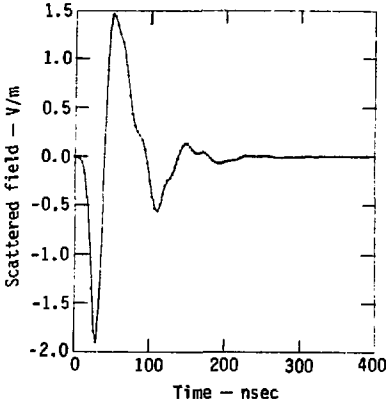

(e) Radiated field vs time ($10/10^3\Omega$ forward/reverse resistance)

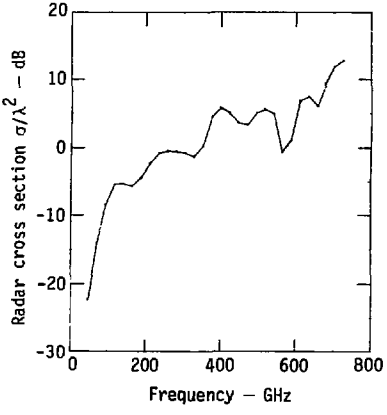

(f) σ/λ^2 vs frequency ($10/10^3\Omega$ forward/reverse resistance)

Fig. 3 (cont.)

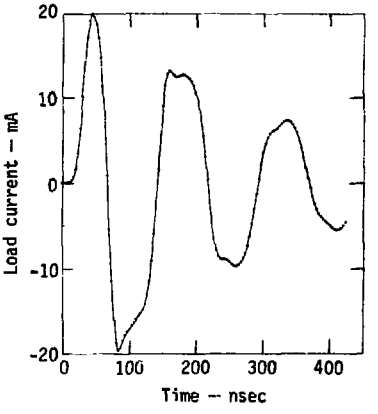

(g) Load current vs time (10/10Ω forward/reverse resistance)

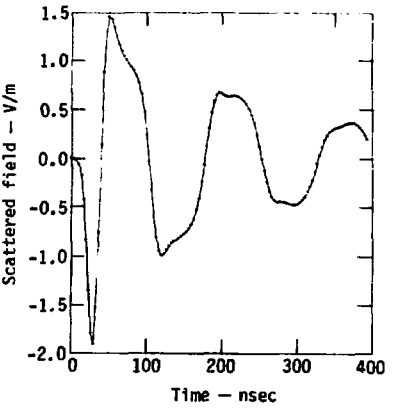

(h) Radiated field vs time (10/10Ω forward/reverse resistance)

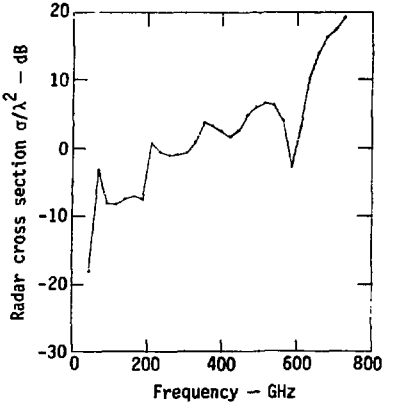

(i) σ/λ^2 vs frequency (10/10Ω forward/reverse resistance)

Fig. 3 (cont.)

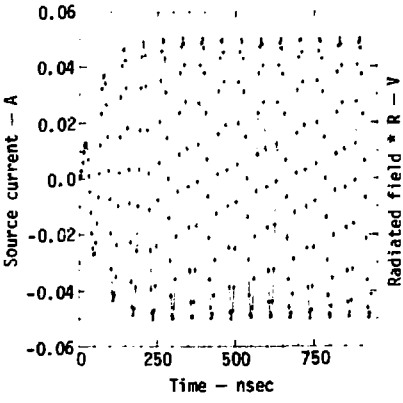

(a) Source current vs time (square-law load)

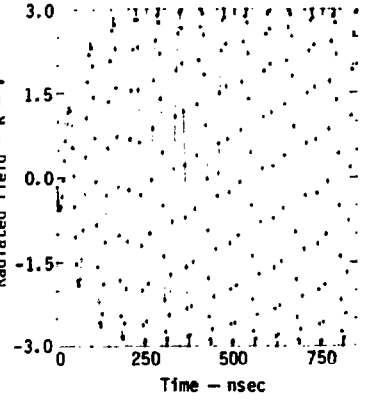

(b) Radiated field * R vs time (square-law load)

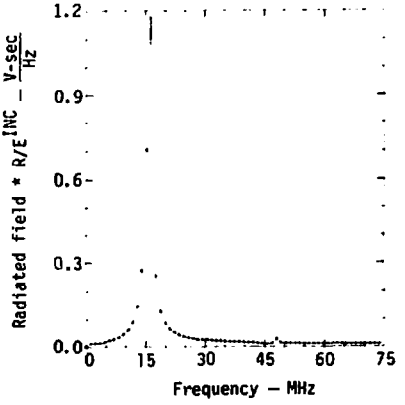

(c) Radiated field * R/E^{INC} vs frequency (square law load)

Fig. 4. Nonlinear impedances, in addition to those with piecewise-linear behavior of the ideal diode, that can be analyzed. In this case, the load resistance is inversely proportional to the voltage magnitude, requiring an iterative solution of Eq. (8) at each time step. Generation of harmonic frequencies for this 9-m, center-excited and loaded antenna is seen in the frequency spectrum.

Gaussian pulse from the square-law load. Other nonlinear loads having essentially arbitrary V-I curves could be readily treated in the same way. For example, when the current is clipped at a 10-mA level, the results shown in Fig. 5 (a) through (c) are obtained; here, the third harmonic component is more pronounced. For comparison, the no-load case is shown in (d) through (f).

Note that clipping the current at a constant level is equivalent to using a time-varying load, whose resistance changes with time in such a way as to keep the load current from exceeding a selected value. Because the time variation is not specified, however, we include this example here instead of in the next section that deals with loads whose time variation is given.

A clipping or current-limiting device is often used to protect circuits from excessive currents or voltages, e.g., in EMP hardening. For this reason, we modeled a 10-m dipole antenna that was illuminated by a normally incident, nominal EMP and loaded at its center by a current-limiting load. The results are shown in Fig. 6. We observe that the load-current spectrum is broadened with respect to the no-load case.

TIME-DEPENDENT LOADS

The use of a time-varying load has some interesting possibilities, including a shifting of the apparent frequency of the scattered field. An example is shown in Fig. 7, in which a 9-m dipole is illuminated by a broadside incidence of a plane-wave Gaussian pulse modulated at 16 MHz. The resistance of the load at the dipole's center varies at a 4-MHz frequency between 0 and 1000 Ω in a square-wave fashion. The time-dependent scattered field is greatly altered from that of the no-lead case, which is shown in Fig. 5 (f) for purposes of comparison. Note the frequency spectrum of the scattered field. Here, appreciable energy is found in the bands that are harmonics of the sum and difference frequencies of the incident field and the

Conclusions

The analysis of nonlinear effects is readily achievable in the time domain. A straightforward modification of a thin-wire time-domain code (WT-MBA/LLL1B)[7] provides a computationally efficient way to analyze various types of nonlinear loads on wire-type structures.

Nonlinearities that can be modeled include arbitrary V-I relationships (among which are diodes, square-law detectors, etc.) and time-varying loads.

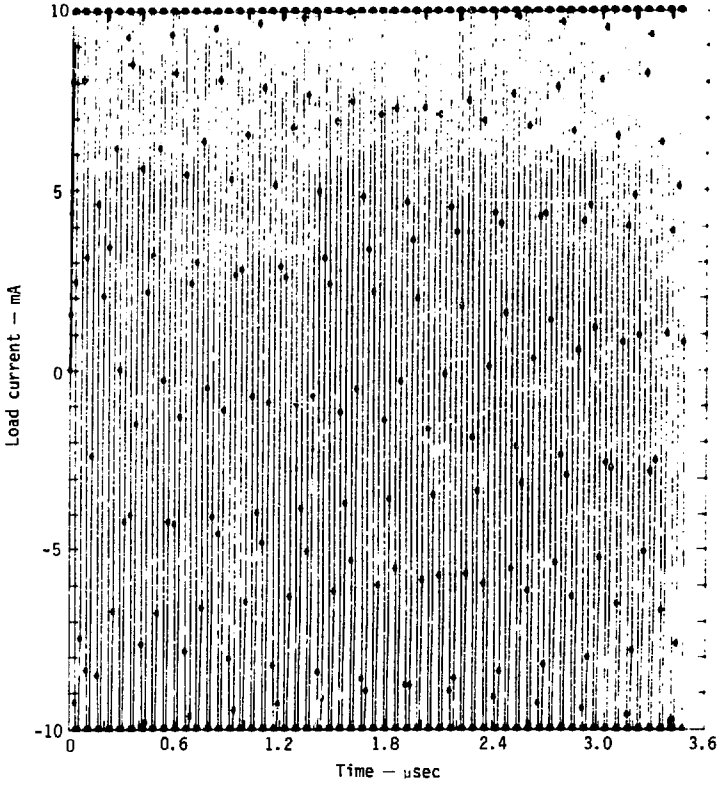

(a) Load current vs time
(current clipped at 10-mA level)

Fig. 5. A current clipper load that can generate frequency harmonics. (a), (b), and (c) show a 9-m dipole with a 10-mA current limiter in series with the source. For comparison, the response of the dipole without the limiter is shown in (d) through (f).

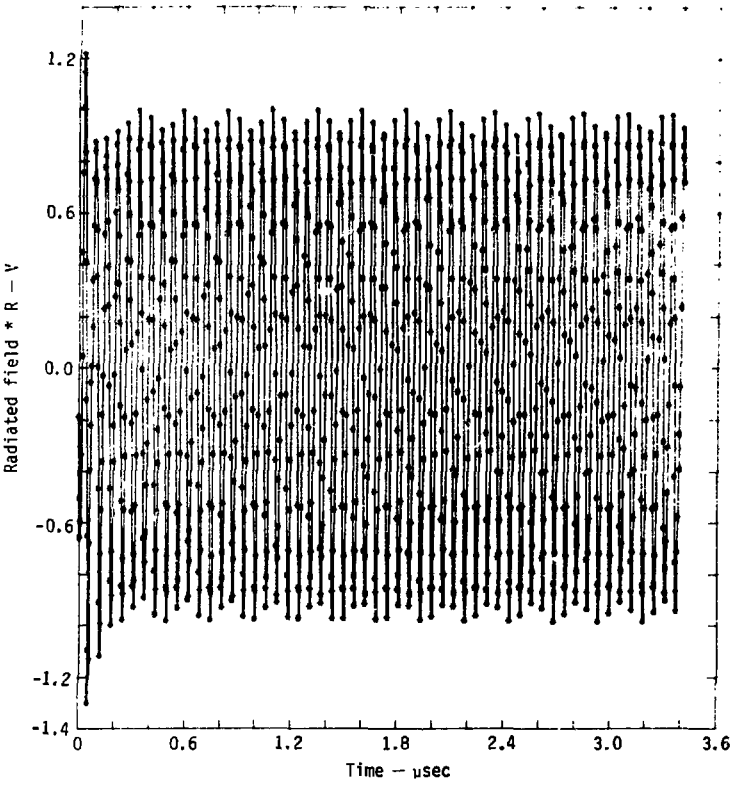

(b) Radiated field * R vs time
(current clipped at 10-mA level)

Fig. 5 (cont.)

(c) E * R magnitude vs frequency (current clipped at 10-mA level)

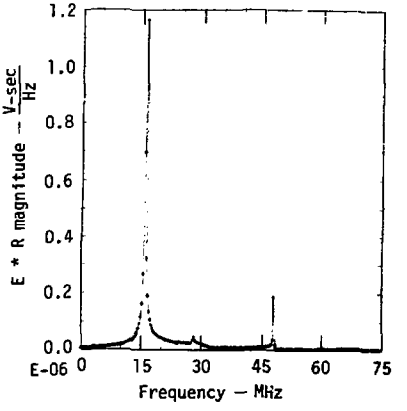

Fig. 5 (cont.)

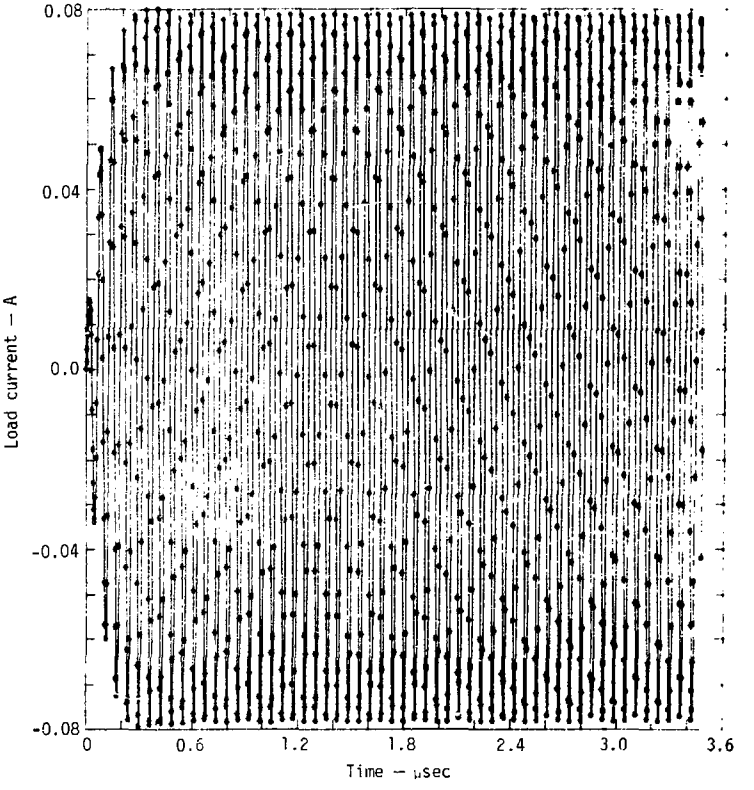

(d) Load current vs time (no load)

Fig. 5 (cont.)

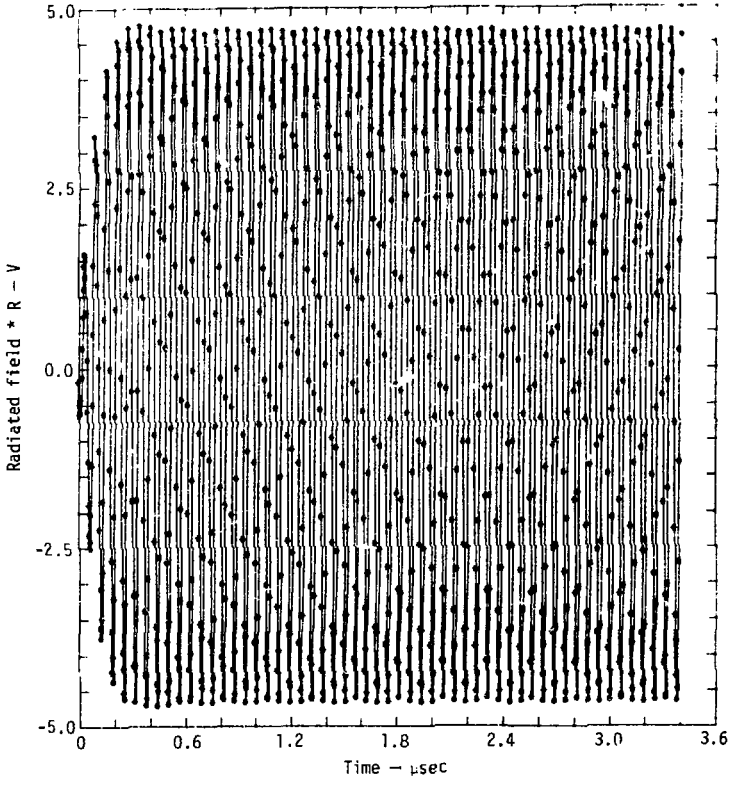

(e) Radiated field * R vs time (no load)

Fig. 5 (cont.)

(f) E * R magnitude vs frequency (no load)

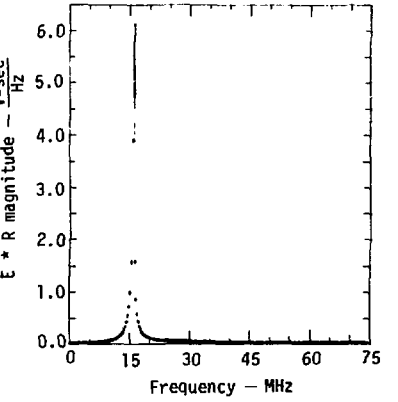

Fig. 5 (cont.)

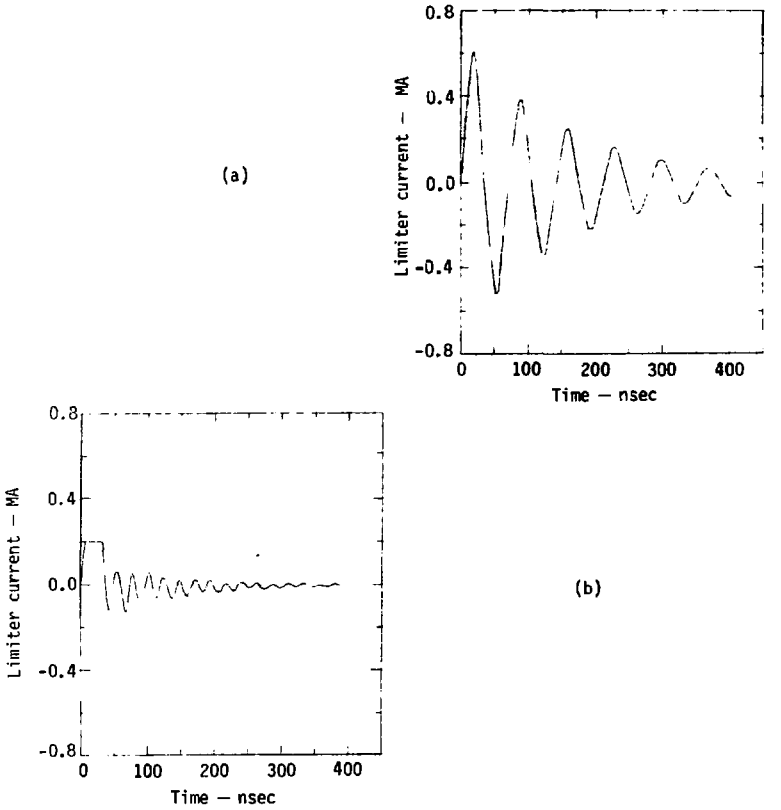

Fig. 6. Action of a current limiter or clipper, illustrated by a 10-m dipole that is illuminated by a broadside incidence EMP. (a) Dipole current when no limiting device is used. (b) Resultant current when a 200-A limiter is inserted at the center of the dipole. Note that the limiter element absorbs much of the dipole energy. (c) & (d) Frequency domain equivalents of (a) and (b), respectively. The action of the limiter tends to broaden the current spectra while decreasing the current component at the half-wave resonance of the unlimited response. (e) Value of limiter resistance as a function of time, where the peak value equals 1280 Ω.

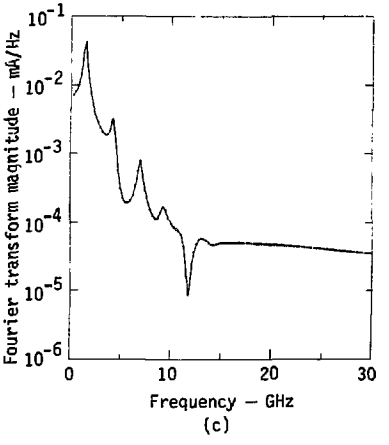

(c)

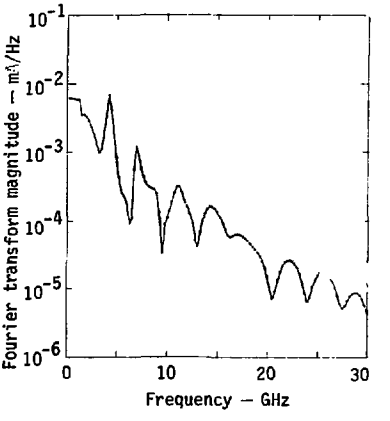

(d)

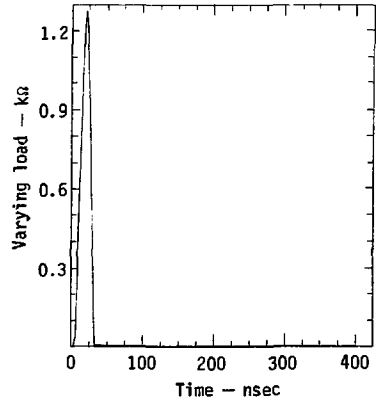

(e)

Fig. 6 (cont.)

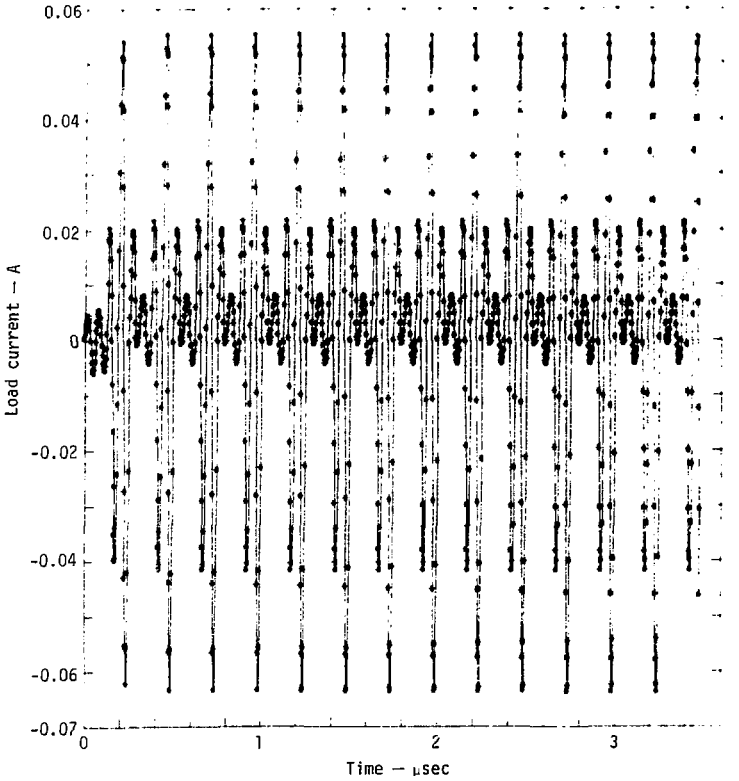

(a) Load current vs time

Fig. 7. Time-varying load in a time-domain computation, illustrated by a 9-m dipole that is illuminated by a broadside incidence of a 16-MHz modulated Gaussian pulse. Load resistance at the center is square-wave modulated. Scattered energy appears in bands, harmonically related to the modulation and illumination frequency. This shows the possibility of scattering signals in desired bands other than the frequency band of the incident signal.

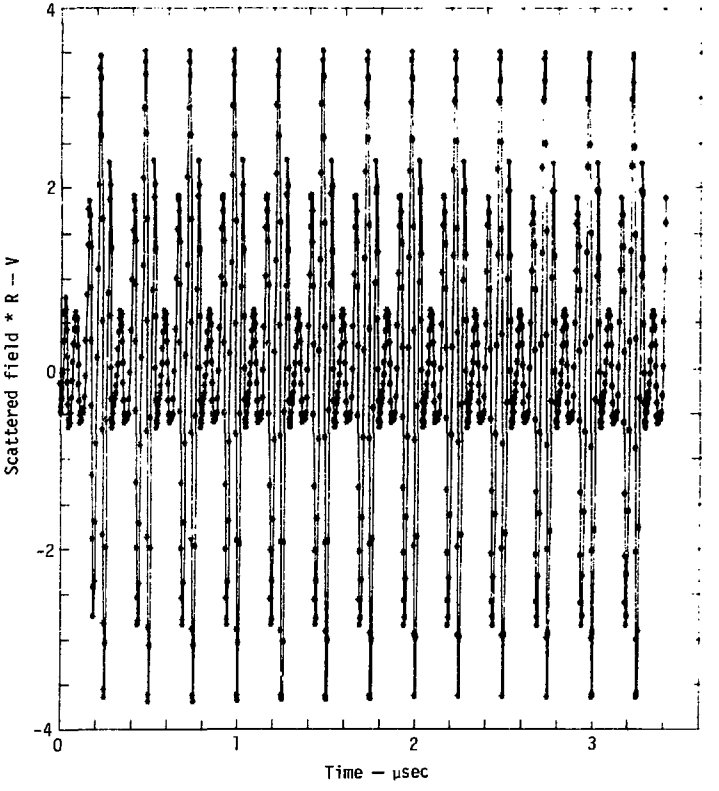

(b) Scattered field * R vs time

Fig. 7 (cont.)

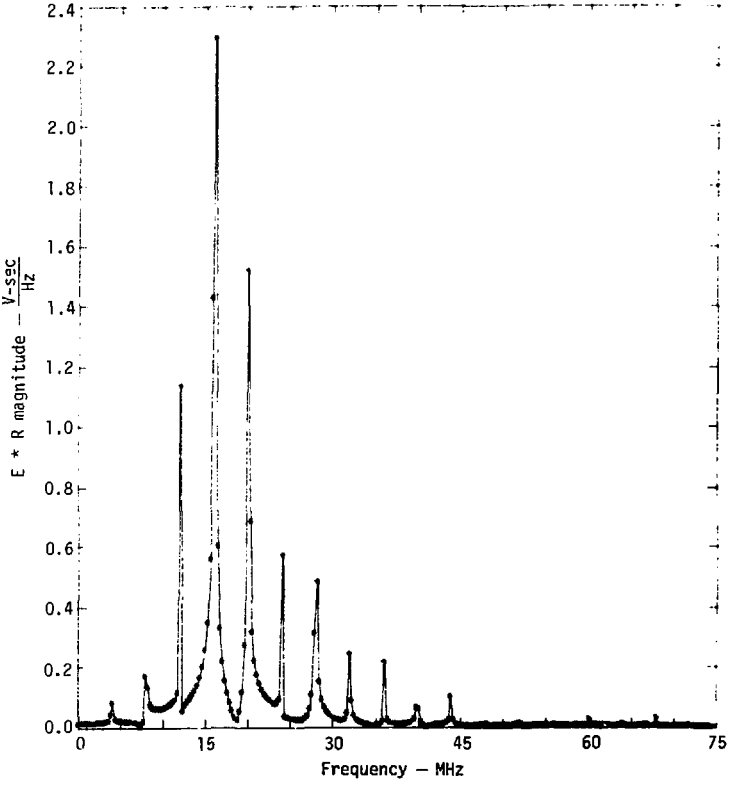

(c) E * R magnitude vs frequency

Fig. 7. (cont.)

We have presented examples of each type. Their applications include: nonlinear behavior resulting from large amplitude excitation (e.g., that caused by EMP and lightning); the influence of protective devices like spark gaps and electrical surge arresters (ESA's); intermodulation resulting from inadvertent nonlinearities (i.e., the "rusty bolt" effect); pulse shaping through the use of diode loads; and spectrum spreading and modification, using time-varying loads.

Acknowledgments

The work reported here was supported in part by the Engineering Research Division of LLL's Electronics Engineering Department and in part by the Defense Nuclear Agency under Subtask R99QAXEB075.

References

1. D. E. Merewether, "Transient Currents Induced on a Metallic Body of Revolution by an Electromagnetic Pulse," *IEEE Trans. Electromagnetic Compat.*, vol. EMC-13, no. 2, 41 (1971).

2. D. E. Merewether and T. F. Ezell, "The Interaction of Cylindrical Posts and Radiation-Induced Electric Field Pulses in Ionized Media," *IEEE Trans. Nucl. Sci.*, vol. NS-21, no. 5, 4 (1974).

3. H. K. Schuman, "Time-Domain Scattering from a Nonlinearly Loaded Wire," *IEEE Trans. Antennas Propagat.*, vol. AP-22, no. 4, 611 (1974).

4. T. K. Liu and F. M. Tesche, "Analysis of Antennas and Scatterers with Nonlinear Loads," *IEEE Trans. Antennas Propagat.*, vol. AP-24, no. 2, 131 (1976).

5. T. K. Sarkar and D. D. Weiner, "Scattering Analysis of Nonlinearly Loaded Antennas," *IEEE Trans. Antennas Propagat.*, vol. AP-24, no. 2, 125 (1976).

6. E. K. Miller, A. J. Poggio, and G. J. Burke, "An Integro-Differential Equation Technique for the Time-Domain Analysis of Thin Wire Structures. I, The Numerical Method," *J. Comput. Phys.*, vol. 12, no. 1, 24 (1973).

7. J. A. Landt, E. K. Miller, and M. Van Blaricum, *WT-MBA/LLL1B: A Computer Program for the Time-Domain Electromagnetic Response of Thin-Wire Structures*, Lawrence Livermore Laboratory, Rept. UCRL-51585 (1974).

BDJ/gw/vt/gw